changes to the far wake. This however, needs further experimental verification.

Conclusion

The measured velocity distribution and velocity defect distribution in the near wake of a flat plate agree fairly well with the values obtained by solving Reichardt's fundamental equation for free turbulence. The momentum transfer coefficient K^2 has the same order of magnitude as obtained by Townsend[12] for circular cylinders. The turbulence intensity variation shows two distinct patterns, one for $\bar{x}=20$ may be the limit at which the near wake changes to the far wake. This however, needs more detailed experimental investigation. The effect of shape parameter H_o at the trailing edge also needs to be investigated further as it seems to have a definite bearing on the wake characteristics.

References

[1]Kiya, M. and Arie M., "An Analysis of Laminar Wake Behind a Symmetrical Two-Dimensional Body in a Uniform Shear Flow," *Bulletin of the JSME*, Vol. 16, Sept. 1973, pp. 1301-1313.

[2]Kiya, M. and Arie, M., "A Perturbation Analysis of the Laminar Far Wake Behind a Symmetrical Two-Dimensional Body in a Uniform Shear Flow," *Journal of Fluid Mechanics*, Vol. 61, Pt. 2, 1973, pp. 305-321.

[3]Talke, F.M. and Berger, S.A., "The Flat Plate Trailing Edge Problem," *Journal of Fluid Mechanics*, Vol. 40, 1970, p. 161.

[4]Schlichting, H., *Boundary Layer Theory*, McGraw Hill, New York, 1960.

[5]Townsend, A.A., *The Structure of Turbulent Shear Flow*, Cambridge University Press, London, 1956.

[6]Toyoda, K. and Hirayama, N., "Turbulent Near Wake of a Flat Plate, Part II," *Bulletin of JSME*, Vol. 18, June 1975, pp. 605-611.

[7]Torda, T.P., Ackermann, W.P., and Burnett, H.R., "Symmetrical Turbulent Mixing of Two Parallel Streams," *Journal of Applied Mechanics*, March 1953, p. 3.

[8]ElAssar, R.J. and Page, R.H., "Incompressible Turbulent Wake of a Flat Plate," *AIAA Journal*, Vol. 7, July 1969, pp. 1388-1389.

[9]Lee, S.C. and Harsha, P.T., "Use of turbulent kinetic energy in free mixing studies," *AIAA Journal*, Vol. 8, June 1970, pp. 1026-1032.

[10]Bradshaw, P., "Prediction of the Turbulent Near Wake of a Symmetrical Aerofoil," *AIAA Journal*, Vol. 8, Aug. 1970, pp. 1507-1508.

[11]Carmody, T., "Establishment of the Wake Behind a Disk," *Transactions of the ASME, Series D*, Vol. 86, 1964, p. 869.

[12]Harsha, P.T. and Lee, S.C., "Correlation Between Turbulent Shear Stress and Turbulent Kinetic Energy," *AIAA Journal*, Vol. 8, Aug. 1970, pp. 1508-1510.

[13]Auiler, J.E. and Lee, S.C., "The Theory of Two-Dimensional Turbulent Wakes," *AIAA Journal*, Vol. 8, Oct. 1970, pp. 1876-1878.

[14]Toyoda, K. and Hirayama, N., "Turbulent Near Wake of a Flat Plate, Part I, Incompressible Flow," *Bulletin of the JSME*, Vol. 17, June 1974, pp. 707-712.

[15]Chevray, R. and Kovasznay, L.S.G., "Turbulence Measurements in the Wake of a Thin Flat Plate," *AIAA Journal*, Vol. 7, 1969, pp. 1641-1643.

[16]Hinze, J.O., *Turbulence*, McGraw Hill, New York, 1959, p. 290.

Modal Synthesis for Combined Structural-Acoustic Systems

Joseph A. Wolf Jr.*

General Motors Research Laboratories, Warren, Mich.

Introduction

THE modal synthesis technique is widely used in structural modeling for dynamics. This method, its history and development are well described in a survey paper presented in 1971 by Hurty.[1] The purpose of this Note is to cast the dynamics of a combined structural-acoustic system in terms of a modal synthesis. This approach appears to be especially useful for determining the low-frequency free and forced interior acoustical properties of the passenger compartments of road and rail vehicles and aircraft wherein the acoustic wavelength is of the same order of magnitude as the dimensions of the structure. As with most such efforts, the goal of this work is to produce cost and time savings in the analysis task. For the examples discussed below, the procedure described herein results in a significant reduction in computer cost from that required for solution of the complete system, with little loss in accuracy.

Received Dec. 13, 1976.

Index categories: Structural Dynamic Analysis; Aircraft Noise, Aerodynamics (including Sonic Boom).

*Senior Research Engineer, Engineering Mechanics Department.

Analysis

Development of the finite element method has produced renewed interest in the structural-acoustic problem by making tractable the solution for arbitrary geometries.[2-8] As a starting point for the present development, we take the equations of motion of the coupled system in the form given by Everstine, et al.[9]

$$\begin{bmatrix} [M_{ss}] & [0] \\ [M_{fs}] & [M_{ff}] \end{bmatrix} \begin{Bmatrix} \{\ddot{u}\} \\ \{\ddot{p}\} \end{Bmatrix} + \begin{bmatrix} [K_{ss}] & [K_{sf}] \\ [0] & [K_{ff}] \end{bmatrix} \begin{Bmatrix} \{u\} \\ \{p\} \end{Bmatrix} = \begin{Bmatrix} \{F_s\} \\ \{0\} \end{Bmatrix} \tag{1}$$

where $\{u\}$ is the vector of n normal displacements for the compartment structure, $\{p\}$ is the vector of m nodal pressures for the enclosed fluid, $[M_{ss}]$ and $[K_{ss}]$ are the $n\times n$ structural mass and stiffness matrices, $[M_{ff}]$ and $[K_{ff}]$ are the $m\times m$ fluid mass and stiffness matrices, $[K_{sf}]=[A]$ and $[M_{fs}]=-(\rho c)^2\ [A]^T$, with $[A]$ a sparse $n\times m$ coupling matrix whose elements are found from the surface area A_{ij} for the boundary node corresponding to the structural displacement u_i and the associated fluid pressure at that node p_j. Also, ρc is the characteristic impedance of the fluid, and $\{F_s\}$ is the vector of external forces applied to the structure.

For brevity, in the remainder of this development, we will consider a free, harmonic solution of Eq. (1), such that $\{F_s\}=\{0\}$ and $\{\ddot{u}\}=-\omega^2\{u\}$, $\{\ddot{p}\}=-\omega^2\{p\}$. The extension to include forced motion can be carried out in the usual way. Furthermore, we will employ a transformation of coordinates, using the structural modes $[\phi_s]$ determined *in vacuo* and the rigid wall acoustic cavity modes $[\phi_f]$, such that

$$\{u\}=[\phi_s]\ \{\eta_s\} \tag{2a}$$

$$\{p\}=[\phi_f]\ \{\eta_f\} \tag{2b}$$

with $\{\eta_s\}$ and $\{\eta_f\}$ representing the appropriate modal coordinates.

Making these substitutions, and premultiplying all terms by

$$\begin{bmatrix} [\phi_s]^T & [0] \\ [0] & [\phi_f]^T \end{bmatrix}$$

gives the desired result

$$-\omega^2 \begin{bmatrix} \lceil M_s \rfloor & [0] \\ -(\rho c)^2[C]^T & \lceil M_f \rfloor \end{bmatrix} \begin{Bmatrix} \{\eta_s\} \\ \{\eta_f\} \end{Bmatrix} + \begin{bmatrix} \lceil K_s \rfloor & [C] \\ [0] & \lceil K_f \rfloor \end{bmatrix} \begin{Bmatrix} \{\eta_s\} \\ \{\eta_f\} \end{Bmatrix} = \{0\} \tag{3}$$

where $[C]=[\phi_s]^T\,[A]\,[\phi_f]$, the modal coupling matrix, and $\lceil M_s \rfloor=[\phi_s]^T\ [M_{ss}]\ [\phi_s]$, etc. Note that the elements of $[C]$ represent the product of the structural "ring" modes with the acoustic cavity modes weighted by the bounding area attributed to each boundary point.

Equation (3) can be solved to establish the natural frequencies and mode shapes of the coupled system. In practice, computational cost and time savings are achieved by retaining only a selected portion of the structural and cavity modes in the solution of Eq. (3). These may be chosen on the basis of a given frequency range of interest, large contributions to the modal coupling matrix, or some other criterion, possibly determined by a computer "experiment" with similar problems. If desired, structural displacements or fluid pressures at points of interest may be determined by means of Eq. (2). These displacements and pressures of interest may also be retained in the synthesis as dependent coordinates, by including the required terms of Eq. (2) as equations of constraint.

Examples

Two examples will be discussed to illustrate the modal synthesis technique. For the first example, we consider the case of a tube of length ℓ and cross-sectional area A, terminated by a rigid, movable plug of mass M supported by a spring with stiffness K, as shown in Fig. 1. The frequencies of this system are the roots of

$$\tan\pi\Omega_s + \mu\Omega_s/\pi(\Omega_p^2 - \Omega_s^2) = 0 \tag{4}$$

where the system frequency ratio $\Omega_s = \omega/\omega_{t1}$, the plug frequency ratio $\Omega_p = \omega_p/\omega_{t1}$, and the mass ratio $\mu = m/M$. The frequency of the combined system is ω, the first frequency of a closed tube $\omega_{t1} = \pi c/\ell$, the frequency of the termination plug $\omega_p = \sqrt{K/M}$ and the mass of enclosed air $m = \rho\ell A$.

For this example, we take the values $\rho = 1.225$ kg/m^3, $c = 340$ m/sec, $\ell = 3.4$ m, $A = 3$ m^2, $\mu = 0.5$, and $\Omega_p = 0.8$. The lowest nonzero roots of Eq. (4) lead to system frequencies of 36.6 and 54.8 Hz. The results of modal synthesis for this problem, including the Helmholtz or uniform pressure "mode" and varying numbers of other closed tube modes are shown in Fig. 1. The errors in the system frequencies are approximately proportional to $1/N$, where N is the total number of closed tube modes included. Although this is not rapid convergence, it should be noted that for engineering purposes, a three- or four-mode model is sufficient.

The second example is a wall and cavity system previously discussed by Dowell and Voss.[10] The flexible wall is a 0.508 m × 0.254 m × 0.127 cm rectangular aluminum plate, covering a cavity whose depth can be varied from 0.051 to 0.305 m. Material properties for the plate are $E = 72.4$ GPa, $G = 27.6$ GPa, $\rho = 2860$ kg/m^3 and for the cavity $c = 343.5$ m/sec, $\rho = 1.225$ kg/m^3.

First, calculate the uncoupled modes and frequencies for the wall and for the cavity. The wall panel has been modeled in NASTRAN with a 5 × 10 element quadrilateral plate mesh covering one-quarter of the panel. The exterior boundaries are given clamped conditions, and the centerline boundaries are constrained to provide symmetric conditions, so that only volume-displacing, symmetric-symmetric (*ss*) modes will be included. Other panel modes are uncoupled from the problem

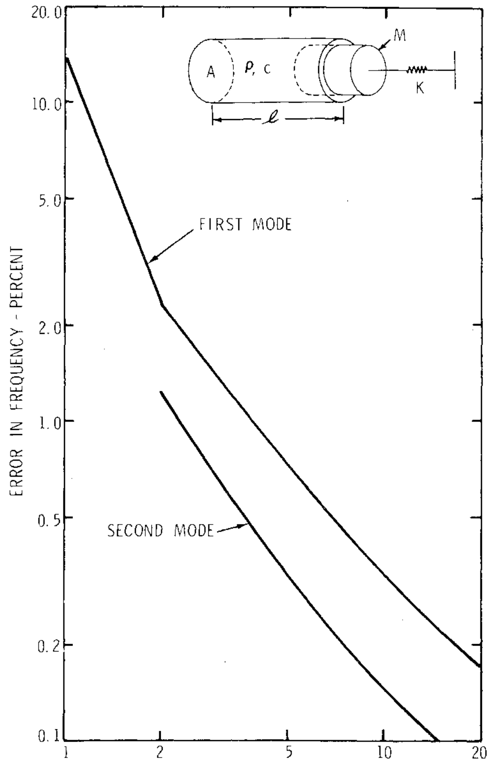

Fig. 1 Frequency convergence for a tube with elastically mounted termination plug.

of interest and will be neglected. The fundamental mode has a frequency of 118 Hz, and the third mode (the next higher *ss* mode) has a natural frequency of 213 Hz. Because of the simple nature of the cavity modes for this example, the rigid wall acoustic frequencies and mode shapes have been calculated directly from theory. Only modes exerting a net pressure on the panel will influence the *ss* modes; other cavity modes are neglected. The first such oscillatory mode occurs at 563 Hz for a 0.305-m deep cavity. The Helmholtz "mode" has also been included in the synthesis.

The cavity effect on panel natural frequencies is shown in Fig. 2 for several length-to-depth ratios. Results of the NASTRAN modal synthesis are compared with the two-term theory of Dowell and Voss[10] for the first two *ss* modes. Two models have been used, the first containing three modes (one cavity and two panel modes) and the second containing all *ss* modes in the range up to 10 times the fundamental panel frequency (five cavity and nine panel modes). The modal solutions yield somewhat higher frequencies than those that Dowell and Voss found. This difference is attributed to the approximate nature of the theory and the slow convergence of the synthesis. Note, however, that increasing the number of included modes from three to 14 produces only a slight improvement in the agreement.

Table 1 Distribution of modal kinetic energy for two modes of combined system

		Substructure modal energy (%)		
System mode	Length/depth ratio	First panel mode	Third panel mode	Helmholtz Cavity "Mode"
	1.67	86.8	0.0	13.2
First mode	3.33	69.2	0.4	30.4
	10.00	54.3	1.5	44.2
	1.67	0.0	97.3	2.7
Third mode	3.33	0.5	90.2	9.3
	10.00	2.1	75.6	22.3

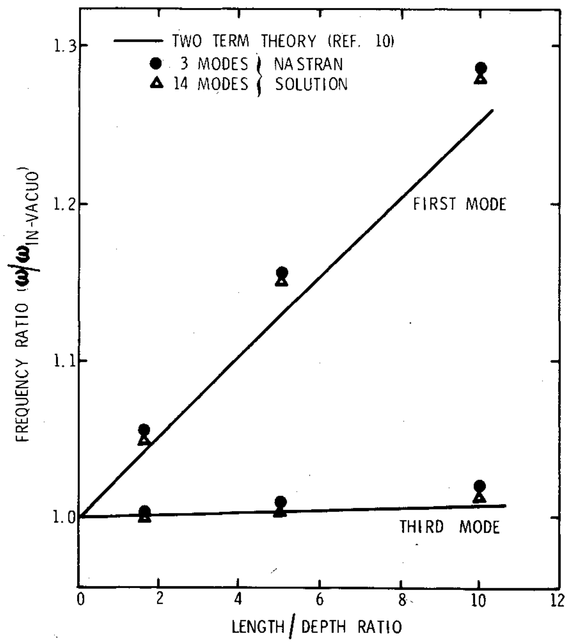

Fig. 2 Cavity effect on panel natural frequencies.

The distribution of modal energies is often of interest in interpreting synthesis results, especially for more complicated structural geometries. For this purpose, the substructure modes are mass normalized prior to inclusion in the synthesis. Then each element of an eigenvector of the synthesis is proportional to the squre root of the kinetic energy in the associated substructure mode. The distribution of kinetic energy in two modes of the panel-cavity system is given in Table 1. The interaction between panel and cavity is greater for a shallower cavity (larger length/depth ratio), as indicated by the increase in energy for the cavity (Helmholtz) mode shown in the last column of Table 1. Note also that for a given length/depth ratio the interaction is greater for the first mode than for the third mode, as mentioned in Ref. 10.

Conclusions

The equations of motion for a combined structural-acoustic system have been reduced to the form of a modal synthesis. This formulation can then be used to economically obtain the system eigenvalues and eigenvectors. These results are of interest in themselves or may serve as the basis for a forced solution.

Acknowledgment

The author acknowledges with pleasure several useful suggestions made by L. J. Howell and D. J. Nefske, who also provided the characteristic equation for the first example.

References

[1]Hurty, W. C., "Introduction to Modal Synthesis Techniques," in *Synthesis of Vibrating Systems*, Neubert, V. H. and Raney, J. P., eds., ASME, New York, 1971, pp. 1-13.

[2]Gladwell, G. M. and Zimmerman, G., "On Energy and Complementary Energy Formulations of Acoustic and Structural Vibration Problems," *Journal of Sound and Vibration*, Vol. 3, 1966, pp. 233-241.

[3]Zienkiewicz, O. C. and Newton, R. E., "Coupled Vibrations of a Structure Submerged in a Compressible Fluid," *Proceedings of the Symposium on Finite Element Techniques*, University of Stuttgart, June 1969, pp. 360-379.

[4]Jennequin, G., "Is the Computation of Noise Level Inside a Car Feasible?," *Proceedings of the Institution of Mechanical Engineers Symposium on Vibration and Noise in Motor Vehicles*, London, 1972, pp. 132-137.

[5]Shuku, T. and Ishihara, K., "The Analysis of the Acoustic Field in Irregularly Shaped Rooms by the Finite Element Method," *Journal of Sound and Vibration*, Vol. 29, 1973, pp. 67-76.

[6]Craggs, A., "An Acoustic Finite Element Approach for Studying Boundary Flexibility and Sound Transmission Between Irregular Enclosures," *Journal of Sound and Vibration*, Vol. 30, 1973, pp. 343-357.

[7]Wolf, J. A., Jr., Nefske, D. J., and Howell, L. J., "Structural-Acoustic Finite Element Analysis of the Automobile Passenger Compartment," SAE Technical Paper 760184, Warrendale, Penn., 1976.

[8]Dowell, E. H., "Acoustoelasticity," in *Advances in Engineering Science, Proceedings of the 13th Annual Meeting of the Society of Engineering Science*, NASA CP-2001, Washington, D.C., 1976, pp. 1057-1070.

[9]Everstine, G. C., Schroeder, E. A. and Marcus, M. S., "The Dynamic Analysis of Submerged Structures," in *NASTRAN: User's Experiences*, NASA TM X-3278, Washington, D.C., 1975, pp. 615-631.

[10]Dowell, E. H. and Voss, H. M., "Experimental and Theoretical Panel Flutter Studies in the Mach Number Range of 1.0 to 5.0," *AIAA Journal*, Vol. 3, Dec. 1965, pp. 2292-2304.

Variable Thickness Shear Layer Aerodynamics Revisited

E. H. Dowell*
Princeton University, Princeton, N.J.
and
M. R. Chi†
NASA Ames Research Center, Moffett Field, Calif.

VENTRES,[1] Chi,[2] and Williams et al.,[3] have studied lifting surface aerodynamics in a parallel, shear flow of constant thickness. To improve the accuracy and realism of this model, particularly in its application to boundary-layer flows, Chi[2] has extended Ventres' solution for this model in steady, two-dimensional incompressible flow to allow for variation of the shear (boundary) layer thickness along the lifting surface chord. His solution, though correct, is unnecessarily elaborate. It is the purpose of the present Note to point out that for shear layers of slowly varying thickness, it is sufficient to replace the constant boundary-layer thickness which appears in Ventres' Kernel function by the varying thickness. The Kernel function in question is that relating pressure on the lifting surface to its downwash (normal velocity on its surface).

Chi[2] has shown for a slowly varying shear layer thickness, $\delta(x)$, that

$$w(x)=\frac{1}{2\pi}\int_{-\infty}^{\infty}K^*[\alpha,\delta(x)]p_w^*[\alpha,\delta(x)]e^{i\alpha x}\mathrm{d}\alpha \tag{1}$$

Here x = coordinate along airfoil chord, w = downwash, K^* = Fourier transform of Ventre's Kernel *for constant* δ with δ now taken as a function of x, and p_w^* = Fourier component of wall pressure. The (physical) wall pressure is given by

$$p_w[x,\delta(x)]=\frac{1}{2\pi}\int_{-\infty}^{\infty}p_w^*[\alpha,\delta(x)]e^{i\alpha x}\mathrm{d}\alpha \tag{2}$$

From Eq. (2), it seems useful to define

$$p_w[x',\delta(x)]\equiv\frac{1}{2\pi}\int_{-\infty}^{\infty}p_w^*[\alpha,\delta(x)]e^{i\alpha x'}\mathrm{d}\alpha \tag{3}$$

Received Dec. 3, 1976.
Index category: Aerodynamics.
*Professor, Department of Aerospace and Mechanical Sciences. Member AIAA.
†NRC Research Associate.